0026-895X/00/061357-11$3.00/0
MOLECULAR PHARMACOLOGY
Copyright © 2000 The American Society for Pharmacology and Experimental Therapeutics
Mol Pharmacol 58:1357–1367, 2000

Vol. 58, No. 6
12772/871787
Printed in U.S.A.

Xenobiotic Transport across Isolated Brain Microvessels Studied by Confocal Microscopy

DAVID S. MILLER, STEPHANIE N. NOBMANN, HEIKE GUTMANN, MICHAEL TOEROEK, JUERGEN DREWE, and GERT FRICKER

Laboratory of Pharmacology and Chemistry (D.S.M.), National Institute of Environmental Health Sciences, National Institutes of Health, Research Triangle Park, North Carolina; Institut fur Pharmazeutische Technologie und Biopharmazie (S.N.N., G.F.), Heidelberg, Germany; Divisions of Gastroenterology and Clinical Pharmacology, Department of Internal Medicine, and Department of Research (H.G., M.T., J.D.), University Clinic (Kantonsspital and Childrens Hospital) Basel, Switzerland

Received June 10, 1999; accepted September 29, 2000

This paper is available online at http://www.molpharm.org

ABSTRACT

To identify specific transporters that drive xenobiotics from central nervous system to blood, the accumulation of fluorescent drugs was studied in isolated capillaries from rat and pig brain using confocal microscopy and quantitative image analysis. Luminal accumulation of daunomycin and of fluorescent derivatives of cyclosporine A (CSA) and ivermectin was concentrative, specific, and energy-dependent (inhibition by NaCN). Transport was reduced by PSC 833, ivermectin, verapamil, CSA, and vanadate, but not by leukotriene C_4 (LTC_4), indicating the involvement of P-glycoprotein. Luminal accumulation of the fluorescent organic anions sulforhodamine 101 and fluorescein methotrexate was also concentrative, specific, and energy-dependent. LTC_4, chlorodinitrobenzene, and vanadate reduced transport of these compounds, but PSC 833 and verapamil did not, indicating the involvement of a multidrug resistance-associated protein (Mrp). Immunostaining localized P-glycoprotein and Mrp2 to the luminal surface of the capillary endothelium and quantitative polymerase chain reaction showed Mrp1 and Mrp2 expression. Finally, the HIV protease inhibitors saquinavir and ritonavir were potent inhibitors of transport mediated by both P-glycoprotein and Mrp. These results validate a new method for studying drug transport in isolated brain capillaries and implicate both P-glycoprotein and one or more members of the Mrp family in drug transport from central nervous system to blood.

The brain capillary endothelium is a formidable barrier to the entry of drugs into the central nervous system. Traditionally, two elements have been considered primarily responsible for the barrier function of this nonfenestrated endothelium: tight junctions, which form an effective seal against intercellular diffusion, and the cells themselves, which exhibit a low rate of endocytosis. More recently, a role in blood-brain barrier function has been proposed for specific drug export pumps (e.g., P-glycoprotein). This proposal is based on three types of evidence. First, Western blots from isolated microvessels and cultured endothelial cell monolayers show a strong signal for P-glycoprotein (Hegmann et al., 1992; Jette et al., 1993; Begley et al., 1996; Huwyler et al., 1996). Immunostaining studies suggest that P-glycoprotein is localized to the luminal surface of the endothelium (Seetharaman et al., 1998), although there is some controversy over this point (see under *Discussion*). Second, cell physiological studies show specific, net basal-to-apical transport of drugs in monolayers of cultured endothelial cells. The transported compounds and the effective inhibitors implicate P-glycoprotein (Tatsuta et al., 1992; Shirai et al., 1994; Huwyler et al., 1996). Third, animals that have reduced P-glycoprotein function as a result of knockout technology or treatment with drugs that saturate or block P-glycoprotein transport activity show increased accumulation of P-glycoprotein substrates in brain as well as a markedly increased sensitivity to neurotoxic P-glycoprotein substrates (e.g., ivermectin) (Schinkel et al., 1994; 1996; Mayer et al., 1997).

Although these findings suggest an important role for the transporter in brain capillary barrier function, there has been no direct demonstration of P-glycoprotein-mediated transport in isolated capillaries. Moreover, it is not clear whether other members of the ABC transporter superfamily also participate. For example, the evidence for Mrp participation comes from experiments with brain capillary endothelial cells in culture (Huai Yun et al., 1998; Regina et al., 1998) and plasma membranes from a brain endothelial cell line (Kusuhara et al., 1998a). However, when brain capillary

Supported by Grant CRG 960281 from the North Atlantic Treaty Organization and DFG FR1211.

ABBREVIATIONS: ABC, ATP-binding cassette; Mrp, multidrug-resistance protein; CSA, cyclosporin A; NBDL, *N*-ε-(4-nitrobenzofurazan-7-yl)-D-Lys8; FL-MTX, fluorescein methotrexate; BO-IVER, bodipy-ivermectin; PCR, polymerase chain reaction; LTC_4, leukotriene C_4; GAPDH, glyceraldehyde-3-phosphate dehydrogenase.

endothelial cells are put into culture, Mrp1 expression increases (Seetharaman et al., 1998), so the physiological significance of the transport experiments with cultured cells is in question. A role for Mrps in barrier function in situ has yet to be established.

A critical impediment to understanding transport function in intact brain capillaries is the lack of suitable in vitro techniques that both retain viability and allow the investigator to measure luminal accumulation of diffusible solutes. For example, although isolated capillaries had been used to study the uptake of radiolabeled glucose and amino acids (Pardridge, 1998), it was not clear from those experiments whether the label accumulated in the cells or in the vascular space. In the present study, we used the optical sectioning capabilities of confocal microscopy to visualize and measure the accumulation of fluorescent drugs within the lumens of freshly isolated capillaries from rat and pig brain. We show that such transport is concentrative, specific, and energy-dependent. Based on substrate and inhibitor profiles and immunostaining experiments, both P-glycoprotein and one or more Mrps seem to be involved. These are the first data to show that transport function of these transporters can be detected in isolated brain capillaries and the first to directly demonstrate a role for an Mrp in the blood-brain barrier.

Materials and Methods

Chemicals. The HIV protease inhibitors saquinavir mesylate and ritonavir were a kind gift from Dr. H. Wiltshire, Roche Ltd., UK. The fluorescent-labeled cyclosporin analog NBDL-CSA was obtained from Novartis LTD, Basel, CH; FL-MTX and BO-IVER were obtained from Molecular Probes (Eugene, OR), and sulforhodamine 101 and daunomycin were obtained from Sigma Chemical (St. Louis, MO). All other chemicals were of analytical grade and were obtained from commercial sources.

Capillary Isolation. Capillaries from pig (2–3 animals per preparation) and rat (3–6 animals per preparation) brain were isolated using a modification of the procedure of Pardridge et al. (1985). All steps in the isolation procedure were carried out at 4°C in pregassed (95% O_2/5% CO_2) solutions. Keeping the tissue on ice and in well-gassed buffers was essential for preservation of transport function. Briefly, pieces of gray matter were gently homogenized in three volumes (v/w) of buffer A (103 mM NaCl, 4.7 mM KCl, 2.5 mM $CaCl_2$, 1.2 mM KH_2PO_4, 1.2 mM $MgSO_4$, 15 mM HEPES) and, after addition of dextran (final concentration 30%), the homogenate was centrifuged at low speed. The resulting pellet was resuspended in buffer B [buffer A supplemented with 25 mM $NaHCO_3$, 10 mM glucose, 1 mM Na-pyruvate, 0.5% (w/v) BSA and then filtered through a 200 μm nylon mesh]. The filtrate was passed over a glass bead column and, after washing with 500-ml buffer, the capillaries adhering to the beads were collected by gentle agitation. Capillaries were centrifuged, the pellet resuspended in ice-cold, gassed, BSA-free Krebs-Henseleit buffer and immediately used for transport experiments.

Confocal Microscopy. To measure transport, 50 μl of capillary suspension was transferred to a covered, Teflon incubation chamber containing 1.5 ml of pregassed Krebs-Henseleit buffer with fluorescent compound and added effectors. The chamber floor was a 4- × 4-cm glass cover slip to which the capillaries adhered and through which capillaries could be viewed by means of an inverted confocal laser microscope. Fluorescent compounds and inhibitors were added to the incubation medium as stock solutions in dimethyl sulfoxide. Preliminary experiments showed that the concentrations of dimethyl sulfoxide used ($\leq$ 0.5%) had no significant effects on the uptake and distribution of the fluorescent labeled test compounds in brain capillaries as measured by confocal microscopy (D.S. Miller, unpublished data). All transport experiments were conducted at room temperature (18–20°C).

The chamber containing tubules was mounted on the stage of a Leica (pig) or Zeiss (rat) inverted confocal laser scanning microscope and viewed through a 63× or 40× water immersion objective (numerical aperture = 1.2). The 568-nm laser line, a 580-nm dichroic filter, and a 590-nm long-pass emission filter were employed for experiments with daunomycin and sulforhodamine 101. A 488-nm laser line, a 510-nm dichroic filter, and a 515-nm long-pass emission filter were employed for experiments with NBDL-CSA, FL-MTX, and bodipy-ivermectin. Low laser intensity was used to avoid photobleaching of the dyes. With the photomultiplier gain set to give an average luminal fluorescence intensity of 100 to 150 (full scale, 255), tissue autofluorescence was undetectable.

To make a measurement, capillaries loaded with fluorescent compound in the chamber were viewed under reduced, transmitted light illumination. A field containing two to five undamaged capillaries was selected and a confocal fluorescence image was acquired and saved. Capillaries for measurement were selected by the following criteria: they contained unbranched segments at least 100 μm in length, appeared undamaged in transmitted light and fluorescence modes, and provided two to three segments in which the optical section was through the widest portion of the vessel. Capillaries were 5 to 8 μm in diameter and pixel resolutions 0.2 μm/pixel. Transmitted light and fluorescence micrographs showed the endothelium to be 1 to 1.5 μm thick.

Fluorescence intensities were measured from stored images using NIH Image 1.61 or Scion Image software as described previously (Miller, 1995). Luminal fluorescence intensity measurements were made of areas within the central 2 μm (10 pixels) of each segment. The background fluorescence intensity was subtracted and the average pixel intensity for each area was calculated. The value used for that capillary was the means of all selected areas. Although some preparation-to-preparation variations in transport ability were noted, most of the differences in fluorescence intensities for control capillaries reflect changes in photomultiplier settings. In previous studies, it has been shown, using video and confocal microscopy and glass capillary tubes filled with solutions of known concentrations of fluorescein, that the relationship between image fluorescence intensity and fluorescein concentration is linear (Miller and Pritchard, 1991; D.S. Miller, unpublished data). However, because there are uncertainties in relating cellular fluorescence to the actual concentration of an accumulated compound in cells and tissues with complex geometry (Sullivan et al., 1990; Miller and Pritchard, 1991), data are reported here as average measured pixel intensity rather than estimated dye concentration.

Immunostaining. Freshly isolated pig and rat brain capillaries adhering to glass cover slips were were washed in PBS and fixed for 10 min at room temperature in 2% (v/v) formaldehyde/0.1% (v/v) glutaraldehyde. After washing in PBS, capillaries were permeabilized in 1% (v/v) Triton X-100 in PBS, washed and incubated for 90 min at 37°C in PBS with primary antibody. After washing, antibody binding was detected using a fluorescein isothiocyanate-labeled secondary antibody for 60 min at 37°C. Capillaries were viewed with a confocal microscope as described above. The primary antibody for P-glycoprotein detection was Ab-1 (Oncogene Science, Uniondale, NY), an antibody to human mdr-1 raised in rabbits. The primary antibody for Mrp detection was a monoclonal antibody to rat cMOAT (Mrp2; kindly provided by Dr. Peter Meier). This antibody does not cross-react with Mrp1 or Mrp6, but its reactivity to Mrp3–5 has not been tested (P. Meier, personal communication).

Real-Time Quantitative PCR. Total RNA was extracted using the RNeasy Mini Kit (Qiagen, Hilden, Germany) according to the manufacturer's protocol. After DNaseI digestion, RNA was quantified using a GeneQuant photometer (Pharmacia, Uppsala, Sweden). Its integrity was checked by ethidium bromide agarose gel electrophoresis. The purity of the RNA preparations was high, as demonstrated by the 260

nm/280 nm ratio (range 1.8 to 2.0). One microgram of total RNA was reverse transcribed by Superscript II (Life Technologies, Basel, Switzerland) according to the manufacturer's protocol using random hexamers as primers. Real-time quantitative PCR analysis was performed with the TaqMan assay using an ABI PRISM 7700 Sequence Detector (PE Biosystems, Rotkreuz, Switzerland), a combined thermocycler and fluorescence detector. A dual-labeled fluorogenic probe complementary to a sequence within each PCR product was added to the PCR reaction. The fluorescent dye at the 5′ end of the probe (6-carboxy-fluorescein) serves as reporter, and its emission is quenched by the second fluorescent dye at the 3′ end of the probe (6-carboxy-tetramethyl-rhodamine). During elongation, the 5′-to-3′ exonuclease activity of the *Taq* DNA polymerase cleaves the probe, thus releasing the reporter from the quencher. Fluorescence is monitored during the whole reaction directly in the reaction tubes. Primers were custom synthesized by Life Technologies (Paisley, Scotland) and probes by Eurogentec (Seraing, Belgium). Primers and probes used were: GAPDH, GGTGAAGGTCGGAGTGAACG and CGACAATGTCCACTTTGCCA with the probe CGCCTGGTCACCAGGGCTGC; MRP1, GACCCTTGATTGCCACGTG and TGGGCTGTGGGAAGTCGT with the probe CCTCCACTTTGTCCATCTCAGCCAAGAG; MRP2, TGTGGGCTTTGTTCTGTCCA and CAGCCACAATGTTGGTCTCG with the probe CTCAATATCACACAAACCCTGAACTGGCTG. Complementary DNA (25 ng total RNA) was amplified in a 25-μl volume containing 12.5 μl of the 2× TaqMan universal PCR master mix (PE Biosystems, Foster City, CA), 225 nM probe, and 900 nM each primer. Cycling conditions were 10 min at 95°C for initial denaturation and activation of AmpliTaq Gold DNA polymerase, followed by 40 cycles at 15 s and 95°C denaturation, and 1-min, 60°C combined annealing and primer elongation. Mathematical analysis was performed as follows: amplification efficiency (E) of individual amplicons were calculated in the exponential phase of the reaction by following equation:

$$E = C_{T1} - C_{T2} \sqrt{\frac{F_{T1}}{F_{T2}}}$$

where C_{T1}, C_{T2} represents the threshold cycles at the threshold fluorescence F_{T1} and F_{T2}, respectively. Quantity of genes were normalized to the constitutive expressed internal control GAPDH by following equation:

$$X_{normalized} = \frac{F_{gene}}{F_{GAPDH}} \times \frac{(1 + E_{GAPDH})^{C_{T,\,GAPDH}}}{(1 + E_{gene})^{C_{T,\,gene}}}$$

where $X_{normalized}$ represents the quantity of the gene normalized to GAPDH.

Data are given as mean ± S.E. Means were considered to be statistically different, when the probability value (P) was less than .05 as measured by unpaired t test.

Results

Figure 1 shows high-magnification bright field and confocal images of a rat brain capillary exposed to 5 μM daunomycin. The bright field image (Fig. 1A) demonstrates the morphological complexities of the preparation. Capillary segments are 5 to 8 μm in diameter and up to several hundred micrometers in length. They can be straight or branched, but their ends appear open. Pericytes are embedded within the capillary endothelium; these are evident as large, oval-shaped cells on the surface. In addition, capillary lumens

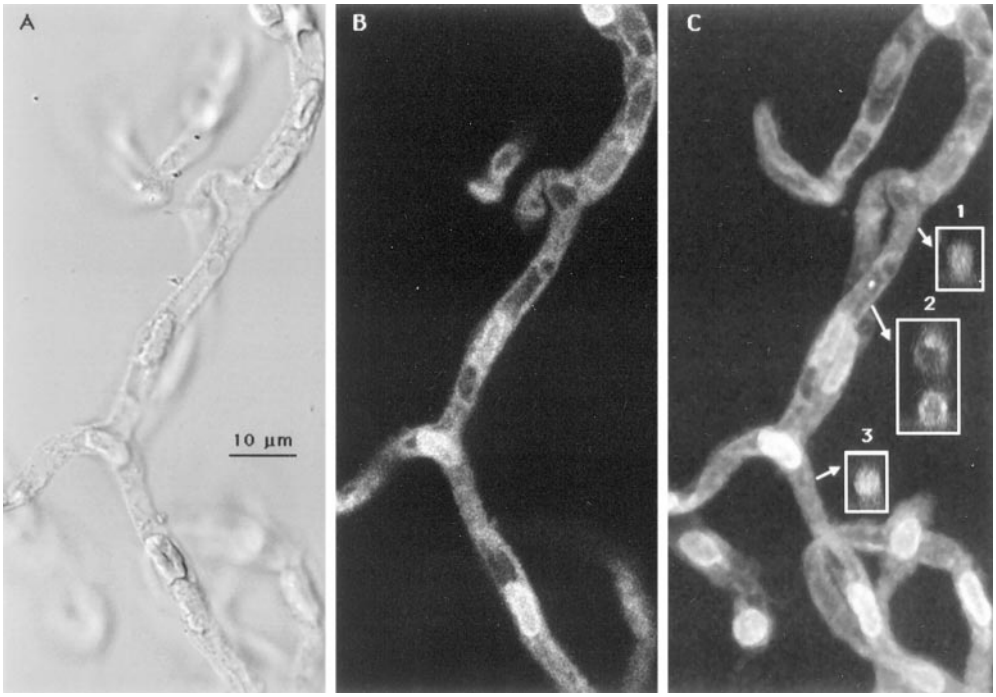

Fig. 1. High-magnification micrographs of rat brain capillaries. Isolated capillaries were incubated for 30 min in medium containing 5 μM daunomycin and then viewed on a confocal microscope. A, transmitted light image of several capillaries with the plane of focus through the topmost. In addition to the capillary endothelium, these vessels contain pericytes within the wall of the capillary and blood cells within the lumen. B, a single confocal section from a stack of 45 images (stack z-spacing, 0.5 μm) taken at roughly the same plane as the transmitted light image. Within the capillary, the regions of highest fluorescence correspond to pericytes and the regions of lowest fluorescence correspond to luminal blood cells. (C) Image constructed from the stack (xyz = 107 × 107 × 22.5 μm) showing all regions of the capillaries in focus (through projection). The arrows indicate the places where stack cross-sections were constructed (z-sections) and each arrow points to the resulting z-section. Z-sections 1 and 3 were taken in areas that were free of pericytes and blood cells. They show a circular, open lumen with a level of fluorescence substantially higher than the medium. Z-section 2 was taken through two capillaries in areas that contain blood cells. In both, luminal fluorescence is much lower than the surrounding endothelium and approaches that of the medium.

contain both a fluid-filled space and blood cells, which can be recognized by their regular, ovoid shape and limiting membranes. Preliminary experiments with fluorescein-labeled dextrans (molecular mass, 10–40 kDa) indicated at best slow penetration of the dye into the luminal space. After 60 to 120 min, levels of fluorescence in the lumen and the endothelium were well below those in the medium (not shown), demonstrating in the isolated capillary that the endothelium presents a significant barrier to the diffusional entry of large molecules, a finding consistent with the known properties of the capillaries in vivo.

Figure 1B is a single confocal slice showing a cross-section of the capillary. Daunomycin fluorescence is not evenly distributed over the vessel. The structures with the highest fluorescence intensity are the pericytes. Our initial estimate from measurements of confocal stacks is that these make up 20% of capillary volume and account for nearly 50% of total fluorescence in vessels exposed to daunomycin. The structures with the lowest fluorescence intensity are the blood cells trapped within the lumen. This can be seen from the single optical slice (Fig. 1B), the reconstructed capillary, and the reconstructed capillary cross sections (Fig. 1C and inset 2), which show that cell-filled areas of the capillaries exhibit little luminal fluorescence. Both the single slice and the reconstructed capillary show that the capillary space not associated with pericytes or blood cells is cylindrical and of intermediate fluorescence (Fig. 1, B and C, and insets 1 and 3). The fluorescence intensity of this space is well above that of the medium. In some parts of the vessel, cellular fluorescence appears somewhat higher than luminal fluorescence.

Figure 2 shows the time course of 5 μM daunomycin accumulation in rat brain capillary lumens. Luminal fluorescence rose rapidly and reached a steady state value within 20 min. At that time, luminal fluorescence was 8 times higher than medium fluorescence, suggesting uphill transport from bath to lumen. Addition of the P-glycoprotein inhibitor PSC-833, to the medium at time 0 reduced steady-state luminal fluorescence by about 70% (Fig. 2); with PSC-833, luminal fluorescence was not significantly different from medium fluorescence. Figure 3 shows micrographs of some of the capillaries from the time course experiment. Note that the PSC 833-treated capillaries exhibited reduced fluorescence within the luminal space along their entire length. In addition, pericyte fluorescence appears somewhat reduced. Initial measurements of cellular fluorescence indicate at most a small reduction by PSC-833 (mean cellular fluorescence intensities averaged 83 $\pm$ 8 and 67 $\pm$ 4 in control specimens and PSC-833-exposed capillaries, $P > .05$).

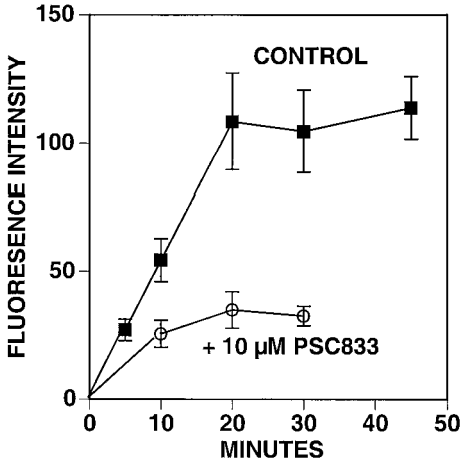

Fig. 2. Time course of daunomycin accumulation in rat brain capillaries. Isolated capillaries were incubated for the time indicated in medium containing 5 μM daunomycin without (control) or with 10 μM PSC 833. Images were collected and analyzed as described under *Materials and Methods*. Each point represents the mean value for five capillaries; variability is given by S.E. bars. At all times, PSC 833 significantly reduced luminal fluorescence ($P < .01$).

Steady-state daunomycin accumulation in capillary lumens was also significantly reduced by verapamil and CSA, both P-glycoprotein substrates, by NaCN, a metabolic inhibitor, and by vanadate, an inhibitor of p-type ATPases. LTC_4, a Mrp substrate that does not affect P-glycoprotein-mediated transport (Kusuhara et al., 1998b), was without effect (Fig. 4). Using brain capillaries from rat and pig, a similar pattern of luminal accumulation and inhibition of that accumulation by P-glycoprotein inhibitors and NaCN was also found for two additional P-glycoprotein substrates: NBDL-CSA, a fluorescent CSA derivative (rat only, Fig. 4), and BO-IVER, a fluorescent ivermectin derivative (rat and pig, Fig. 5).

In initial experiments directed at determining whether isolated brain capillaries could also transport organic anions, we found evidence for specific luminal accumulation of three dyes, FL-MTX, FLUO-3, and sulforhodamine 101. Because of its resistance to photobleaching and the insensitivity of fluorescence to changes in pH, sulforhodamine 101, a disulfonic acid, was chosen as primary test substrate. Figure 6 shows confocal images of a rat brain capillary incubated in medium containing 1 μM sulforhodamine 101. As with the P-glycoprotein substrates, this organic anion accumulated in the pericytes and the luminal space, but not within blood cells. The fluorescence intensity of the luminal compartment was substantially higher than that of the medium.

Endothelial cells seemed to concentrate the compound within a punctate compartment, near the luminal membrane (Fig. 6). Consequently, the luminal spaces in capillaries loaded with sulforhodamine 101 are better defined than in capillaries loaded with daunomycin (compare Figs. 1 and 6). Experiments with renal cells in culture have shown that sulforhodamine 101 accumulates in mitochondria (D.S. Miller, unpublished data) and our preliminary experiments with rhodamine 123-loaded brain capillaries show a pattern of punctate, cellular fluorescence similar to that seen with sulforhodamine 101, suggesting mitochondrial accumulation.

When isolated brain capillaries from rat and pig were exposed to media with 1 to 5 μM sulforhodamine 101, luminal fluorescence intensity rose rapidly with time and, within 10 to 15 min, reached a steady-state value 3 to 5 times that of the medium (not shown). Steady-state luminal fluorescence in rat and pig brain capillaries was greatly reduced when metabolism was inhibited by 1 mM NaCN (Fig. 7). Compounds that affect transport on Mrps also reduced luminal accumulation of sulforhodamine 101. These included 300 to 500 nM LTC_4, 5 μM CSA, and 50 μM vanadate. In contrast to experiments with P-glycoprotein substrates, verapamil, and PSC 833 (at 10 μM) were without significant effect (Figs. 7 and 8). In limited experiments with FL-MTX (Fig. 8) and FLUO-3 (data not shown) similar inhibitory effects of NaCN and LTC_4 were found, suggesting that all three fluorescent organic anions shared a common transport pathway.

We used two methods to detect expression of ATP-driven drug export pumps in brain capillaries. First, capillaries from control and TR− rats (a strain that does not express Mrp2; Konig et al., 1999) were fixed, permeabilized, and incubated with nonfluorescent antibodies to P-glycoprotein and to Mrp2 (antibody may also recognize Mrp3 and Mrp5). Antibody-antigen association was detected with fluorescent secondary antibodies. Figure 9 shows representative confocal images of immunostained capillaries. In capillaries from control rats, both antibodies labeled structures that line the capillary lumens, indicating localization to the luminal surface of the endothelial cells. In addition, Fig. 9B shows that P-glycoprotein is localized to punctate sites at or near the basal surface of the endothelial cells. In capillaries from TR− rats, P-glycoprotein labeling was similar to that seen with controls (not shown); however, specific labeling of Mrp2 was absent (Fig. 9E).

Second, we used real time quantitative PCR (see under *Materials and Methods*) to detect and measure levels of Mrp1 and Mrp2 mRNA in gray cortex of rat brain and in isolated rat brain capillaries. Mrp1 and Mrp2 mRNA levels normalized to GADPH were 0.003 ± 0.005 and 0.149 ± 0.021,

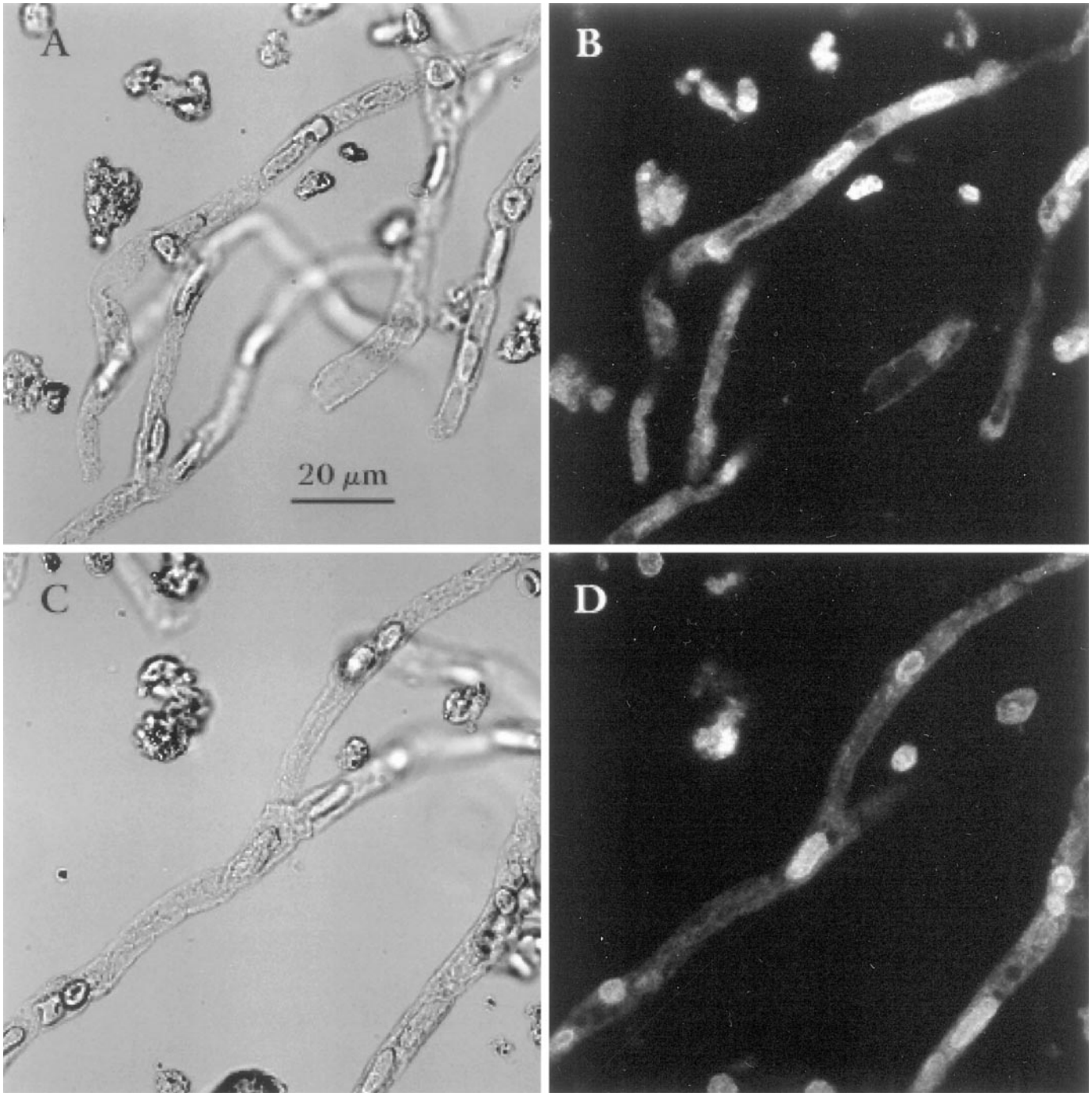

Fig. 3. Effect of PSC 833 on daunomycin accumulation. Transmitted light (A and C) and confocal (B and D) micrographs of rat brain capillaries after 30 incubation in media containing 5 μM daunomycin without (A and B) and with 10 μM PSC 833 (C and D). Notice the reduction in luminal fluorescence in the capillaries exposed to PSC 833.

respectively, for gray cortex and 0.054 ± 0.004 and 0.378 ± 0.046, respectively, for isolated capillaries (data from three to four preparations). Clearly, expression of Mrp1 and Mrp2 could be detected in isolated capillaries and levels in that preparation were higher than in overall brain tissue.

One limitation in the use of HIV-1 protease inhibitors is

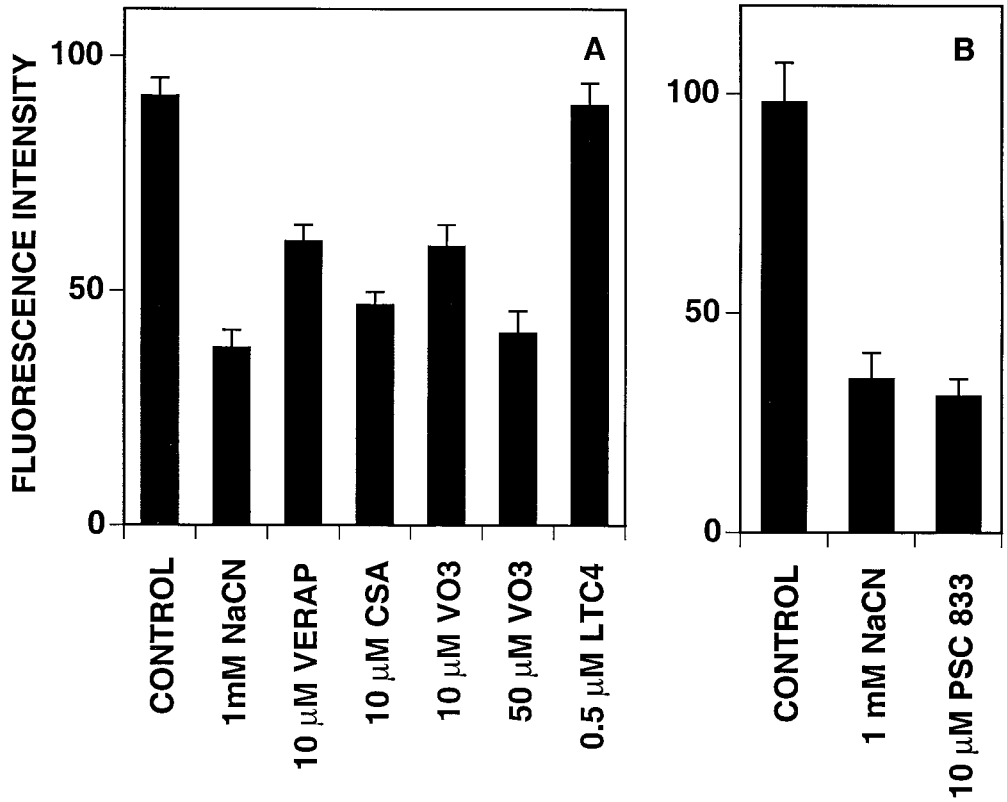

Fig. 4. Inhibitors of daunomycin (A) and NBDL-CSA (B) transport. Isolated rat brain capillaries were incubated for 30 min in medium containing 5 μM daunomycin or 1 μM NBDL-CSA without (control) or with the indicated additions. Images were collected and analyzed as described under *Materials and Methods*. Data given as mean ± S.E. for 18 to 37 capillaries from two preparations. With the exception of LTC_4, all additions significantly reduced luminal fluorescence ($P < .01$).

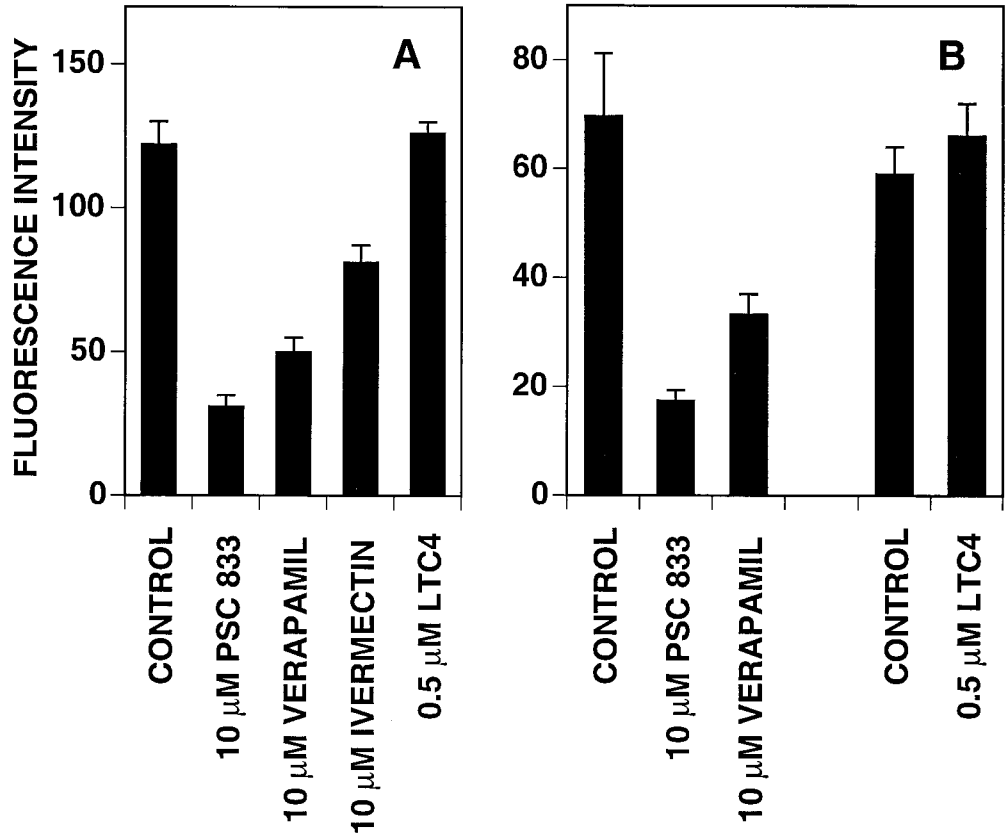

Fig. 5. Inhibitors of bodipy-ivermectin transport. Isolated rat (A) and pig (B) brain capillaries were incubated for 30 min in medium containing 1 μM bodipy-ivermectin without (control) or with the indicated additions. Images were collected and analyzed as described under *Materials and Methods*. Data given as mean ± S.E. for 15 to 32 capillaries from two rat and one pig preparations. With the exception of LTC_4, all additions significantly reduced luminal fluorescence ($P < .01$).

their inability to cross the blood-brain barrier and act at sites of infection within the central nervous system. P-glycoprotein-mediated transport at the blood-brain barrier has been implicated in the near-exclusion of saquinavir and other HIV-1 protease inhibitors from the central nervous system (Glynn and Yazdanian, 1998; Kim et al., 1998; Drewe et al., 2000) and recent experiments indicate that Mrp2 might also participate (Gutmann et al., 1999a). To determine whether the HIV protease inhibitors saquinavir and ritonavir interacted with drug transporters in brain capillaries, we incubated isolated capillaries from pig in media without (control) or with saquinavir and ritonavir. Figure 10 shows that these HIV-1 protease inhibitors were potent inhibitors of the transport of both BO-IVER and sulforhodamine 101 from bath to capillary lumen. With BO-IVER as substrate, 0.1 μM ritonavir reduced luminal accumulation by about 35% (Fig. 10A). With sulforhodamine 101 as substrate, both ritonavir and saquinavir reduced luminal accumulation in a concentration-

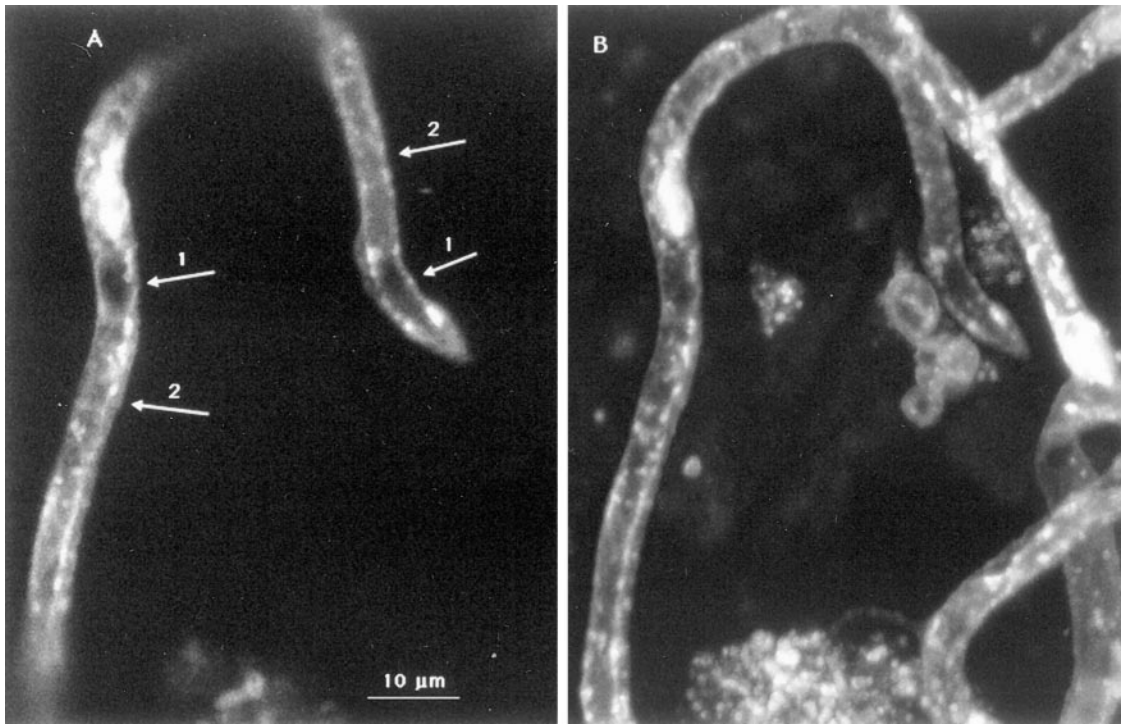

Fig. 6. Confocal images of rat brain capillaries after 30 incubation in medium containing 1 μM sulforhodamine 101. A, a single confocal section from a stack of 62 images (stack z-spacing, 0.5 μm). Within the capillary, the regions of highest fluorescence correspond to pericytes and the regions of lowest fluorescence correspond to luminal blood cells (arrows 1). Regions of capillary endothelium without pericytes or blood cells are of intermediate fluorescence (arrows 2) but are still more fluorescent than the medium. B, image reconstructed from the stack showing all regions of the field in focus (through projection).

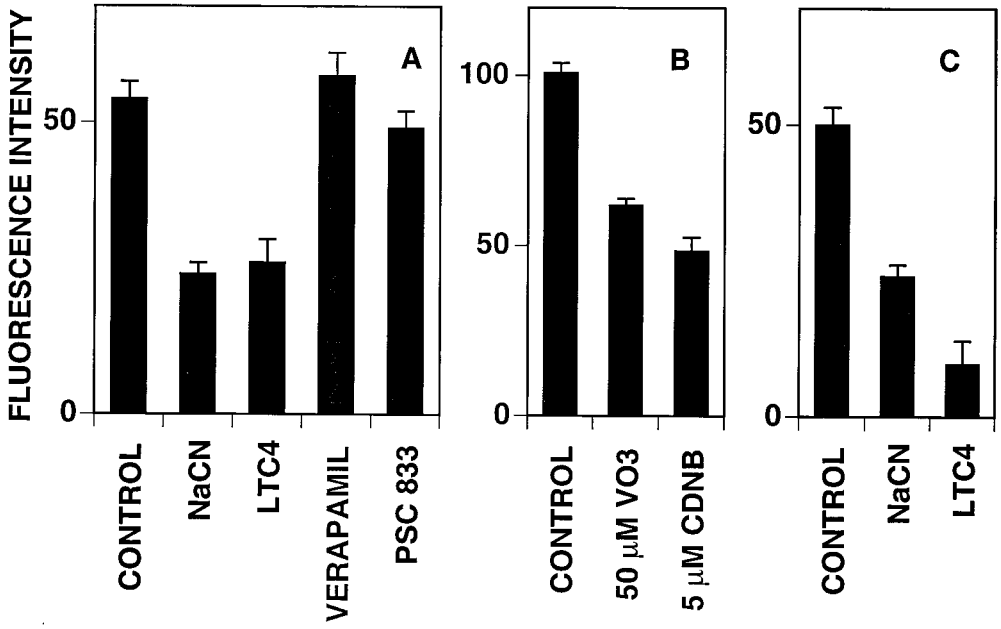

Fig. 7. Inhibitors of sulforhodamine 101 (A and B) and fluorescein-methotrexate; C) transport in rat brain capillaries. Isolated capillaries were incubated for 30 min in medium containing 1 μM sulforhodamine 101 or 1 μM FL-MTX without (control) or with the indicated additions. Images were collected and analyzed as described under *Materials and Methods*. Data given as mean ± S.E. for 15 to 28 capillaries from one preparation. With the exception of verapamil and PSC 833, all additions significantly reduced luminal fluorescence ($P < .01$).

dependent manner (Fig. 10B). Of the two drugs, ritonavir was clearly the more potent inhibitor, causing significant reduction of sulforhodamine 101 transport into the lumen at concentrations as low as 10 nM and 50% inhibition at 50 nM (Fig. 10B). Preliminary measurements showed that ritonavir altered transport at the luminal membrane of the endothelium, because cellular fluorescence intensity did not decrease (mean values for 7–10 capillaries were: controls, 106 ± 6; 10 nM ritonavir, 99 ± 12; 50 nM ritonavir, 105 ± 6; 500 nM ritonavir, 100 ± 15).

Discussion

The present report introduces a new approach to studying excretory (central nervous system to blood) transport in freshly isolated, intact brain capillaries: the use of fluorescent substrates, confocal microscopy and quantitative image analysis. The advantage of this approach is one of spatial resolution. Using the optical sectioning capabilities of confocal optics, substrate fluorescence in the capillary lumen can be distinguished from that in the endothelium and associated cells and the fluorescence intensities of the luminal compartment and the medium can be measured and compared. Micrographs of these capillaries show them to be several hundred micrometers long with an open luminal space (best seen in tubules incubated in medium with sulforhodamine 101; Fig. 6). Although the ends of the segments appear to be open to the medium and are thus potential sites of diffusional leakage, we expect that this leakage is minimized by the long diffusion distances involved and the fact that the luminal compartment is both narrow and unstirred. Our experiments showing long-term exclusion of fluorescent dextrans from the lumen support this supposition. At present, a major limitation of the system is limited viability, a problem that was noted previously (Sussman et al., 1988). Nevertheless, for a period of 2 to 4 h after isolation, the capillaries both excluded fluorescent dextrans and supported xenobiotic transport from bath to lumen that was concentrative, specific, and metabolism-dependent (reduced by NaCN). Thus, both the barrier and specific transport functions of the endothelium were at least partially preserved. Experiments are currently under way to define conditions that will optimize the metabolic viability of the capillaries.

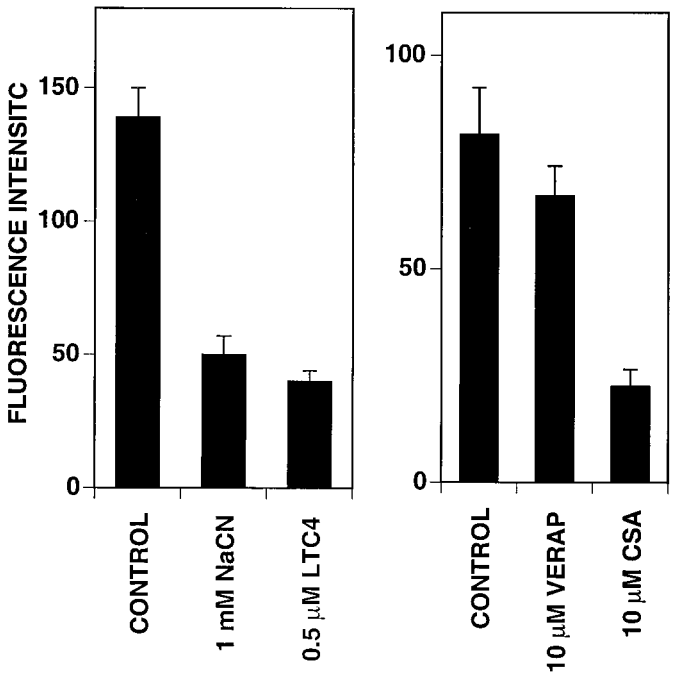

Fig. 8. Inhibitors of sulforhodamine 101 transport in pig brain capillaries. Isolated capillaries were incubated for 30 min in medium containing 1 μM sulforhodamine 101 without (control) or with the indicated additions. Images were collected and analyzed as described under *Materials and Methods*. Two experiments are shown. Data given as mean ± S.E. for 12 to 22 capillaries from one preparation. With the exception of verapamil, all additions significantly reduced luminal fluorescence ($P < .01$).

Here we used isolated capillaries from rat and pig to investigate directly the mechanisms by which selected fluorescent xenobiotics are transported from bath to lumen. Fluorescent compounds were chosen based on previous transport and immunolocalization studies, primarily in isolated renal proximal tubules, that showed uphill cell to tubular lumen transport mediated by either P-glycoprotein (daunomycin, NBDL-CSA and BO-IVER) (Miller, 1995; Schramm et al., 1995; Fricker et al., 1999) or Mrp2 (sulforhodamine 101 and FL-MTX; Masereeuw et al., 1996, 2000) and specific labeling of the luminal membranes of the tubular epithelial cells with antibodies to mammalian P-glycoprotein and Mrp2 (Masereeuw et al., 2000; D.S. Miller, unpublished data). Also, Fl-MTX has been shown to be a potent inhibitor of Mrp2-mediated transport in vesicles from insect cells expressing rabbit Mrp2 (Van Aubel et al., 1998). In the present study, luminal accumulation of all fluorescent substrates was found to be rapid, metabolism-dependent, and specific. Vanadate reduced the transport of both daunomycin and sulforhodamine 101, suggesting the involvement of p-type ATPases. Note that with all substrates, the reduction of luminal accumulation was not total. Even with the most potent inhibitors of transport, 30 to 40% remained. It is not clear at present whether this is a reflection of the experimental protocol (i.e., transport of lipophilic substrates from an infinite bath), the reduced metabolic competence of the capillaries, or reduced temperature (18–20°C versus 37°C in vivo).

Luminal accumulation of daunomycin, NBDL-CSA, and BO-IVER was reduced by several P-glycoprotein substrates and modifiers, including PSC 833, CSA, verapamil and ivermectin, but not LTC_4, an inhibitor of transport mediated by Mrps but not P-glycoprotein. These data for transport of daunomycin, NBDL-CSA, and BO-IVER and their inhibition by drugs known to interact with P-glycoprotein indicate that this transporter participates in xenobiotic transport across the capillary endothelium. Based on these results, the simplest transport model would place P-glycoprotein on the luminal membrane of the endothelial cells, in the correct location to use ATP to both pump xenobiotics from cell to blood and prevent entry into the central nervous system. The present immunostaining experiments support this luminal placement. There has been some controversy regarding the immunolocalization of P-glycoprotein in human brain capillaries. Work from the Pardridge laboratory indicates localization of the transporter to pericytes (Pardridge et al., 1997; Golden and Pardridge, 1999), whereas other laboratories show localization to the endothelial cells (Jette et al., 1993; Seetharaman et al., 1998). The present results for rat and pig are consistent with the latter, but they also suggest a secondary localization of P-glycoprotein to sites on the basal surface of the capillary. At present, it is unclear whether

these sites are on the basal membrane of the endothelial cells or are remnants of associated cells removed during capillary isolation.

In contrast to the P-glycoprotein substrates, luminal accumulation of the fluorescent organic anions sulforhodamine 101 and FL-MTX was not reduced by verapamil or PSC 833. At the 10 μM concentration used, one would expect that these compounds would block transport mediated by P-glycoprotein. Luminal accumulation of sulforhodamine 101 and FL-MTX was reduced by low concentrations of LTC_4 and

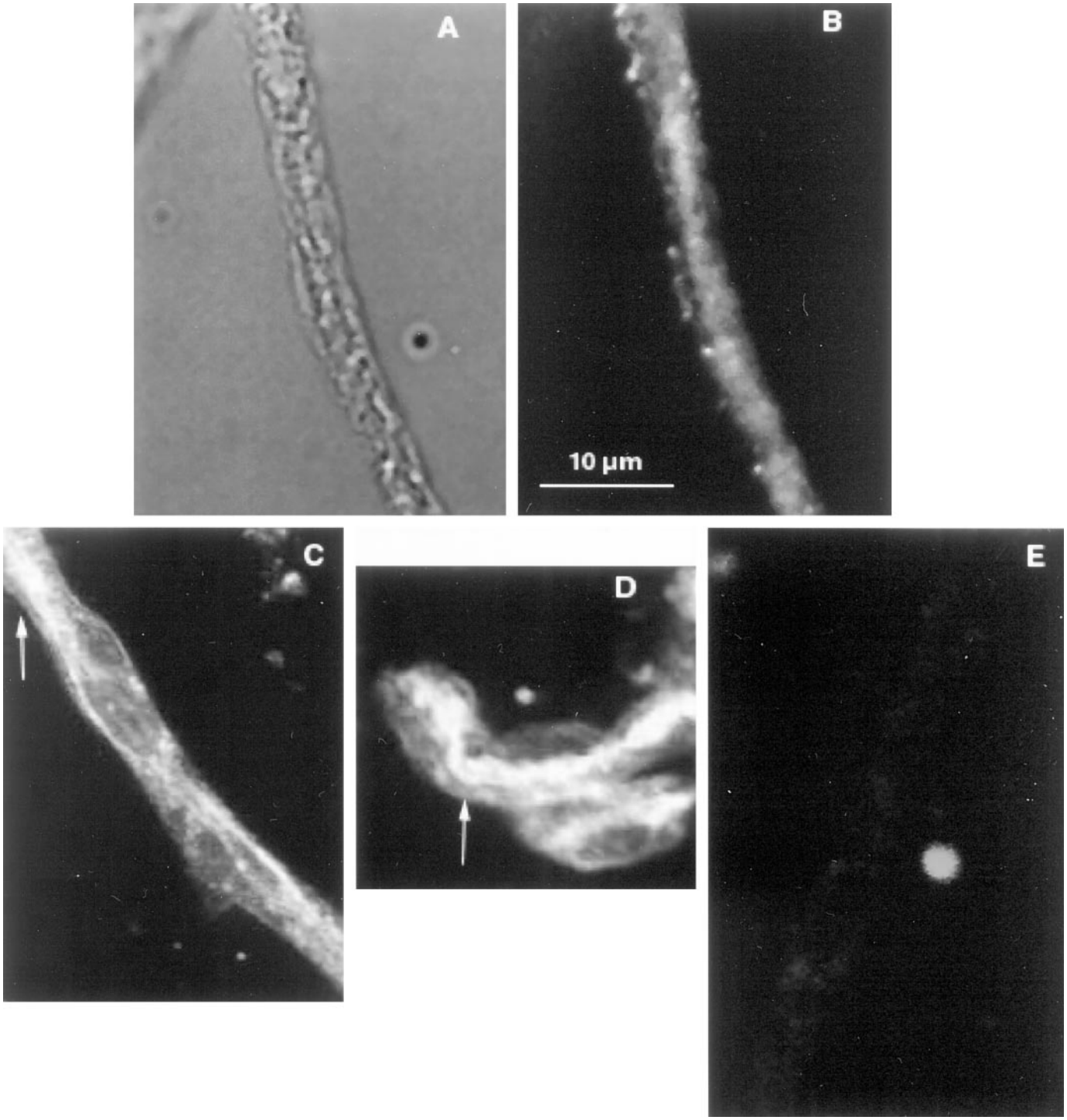

Fig. 9. Confocal immunolocalization of P-glycoprotein and Mrp2 in rat brain capillaries. Capillaries were processed as described under *Materials and Methods* and exposed to a polyclonal anti-P-glycoprotein antibody (A, transmitted light image; B, fluorescence) or a monoclonal, anti-Mrp2 antibody (C–E) followed by a fluorescein isothiocyanate-labeled secondary antibody. Control experiments in which primary antibodies were omitted showed little tissue autofluorescence and nonspecific binding of secondary antibody. C and D show staining in capillaries from control rats; E shows staining in capillaries from TR− rats, a strain that does not express Mrp2 (Konig et al., 1999). Note that the capillary lumens are partially collapsed. Both antibodies stain primarily a structure within the capillary. This structure runs through the length of the capillary and seems to correspond to the luminal surface of the endothelium (arrows). The anti-P-glycoprotein antibody may also stain structures on the surface of the capillary. No Mrp2 staining is seen in capillaries from TR− rats.

CDNB. This is similar to the transport and inhibition pattern for these substrates seen in teleost renal proximal tubule. In that tissue, based on transport inhibitor studies and immunostaining with antibodies to mammalian transporters, cell to lumen transport of FL-MTX was attributed to Mrp2 (Masereeuw et al., 1996, 2000), an Mrp isoform that is known to be highly expressed in proximal tubule (Schaub et al., 1997). So far, however, six Mrp isoforms have been cloned. They exhibit isoform-specific tissue expression patterns, but it is not clear from the limited data available whether individual isoforms can be distinguished based on substrate or inhibitor specificity patterns (Konig et al., 1999). The present transport data for brain capillaries suggest the involvement of one or more of these Mrps in the luminal accumulation of organic anions. However, two additional observations are consistent with participation of Mrp2. First, immunostaining with an antibody raised to Mrp2 (but that may also react with Mrp3–5) showed exclusive localization at the luminal membrane of the endothelial cells in capillaries from control rats, but no staining in capillaries from TR− rats; the latter strain does not express Mrp2 (Konig et al., 1999). Second, quantitative PCR detected Mrp1 and Mrp2 mRNA in rat brain cortex and isolated capillaries. Together, these findings implicate Mrp2 (and possibly other Mrps) in the cell-to-lumen transport of anionic xenobiotics in brain capillaries.

Finally, we have used the new experimental system to examine briefly in pig brain capillaries the sensitivity of P-glycoprotein and Mrp to inhibition by the HIV-1 protease inhibitors saquinavir and ritonavir. Both drugs have been shown to be secreted in monolayers of CACO-2 cells, which express both P-glycoprotein and Mrp2 (Gutmann et al., 1999b). In these cells, saquinavir and ritonavir secretion was partially blocked by P-glycoprotein inhibitors, but the effects of Mrp2 inhibitors were not tested. We recently examined the interactions of these protease inhibitors with drug transporters in renal proximal tubule and found that they were potent inhibitors of transport mediated by both P-glycoprotein and Mrp2 (Gutmann et al., 1999a). The present results show that ritonavir, at submicromolar concentrations, substantially reduced the transport of both BO-IVER and sulforhodamine 101. Saquinavir was used only in experiments in which sulforhodamine 101 transport was assayed; it also inhibited transport, but at much higher concentrations than ritonavir. In two important respects, these results agree with those obtained from renal proximal tubules: 1) the protease inhibitors interacted with both P-glycoprotein and one or more Mrps, and 2) ritonavir was by far the most potent inhibitor of the two, being as effective as the best of the known P-glycoprotein and Mrp inhibitors. These preliminary results suggest that transport by P-glycoprotein and an Mrp underlies in part the poor penetration of the blood-brain barrier by HIV protease inhibitors. As in the renal tubule (Gutmann et al., 1999a), the inhibitory potency of ritonavir suggests uses for this drug outside of HIV therapy (e.g., in reversing drug resistance caused by ABC transporters).

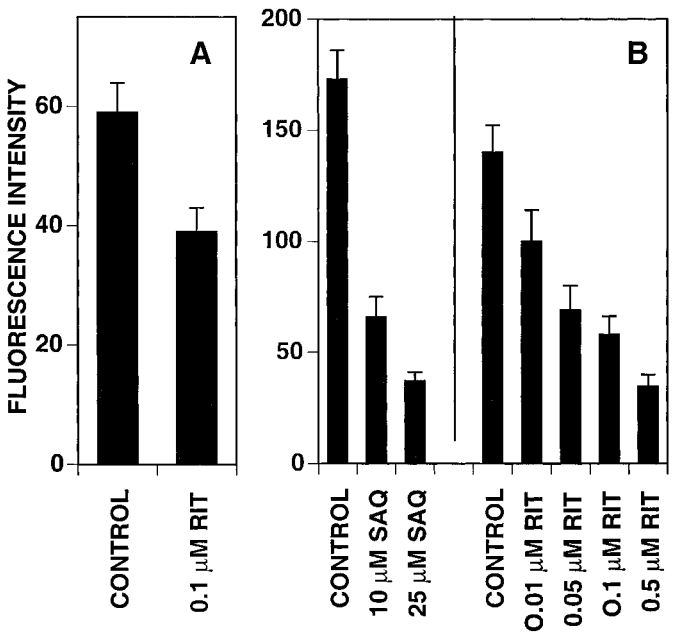

Fig. 10. Effects of ritonavir and saquinavir on transport of bodipy-ivermectin (A) and sulforhodamine 101 (B) in pig brain capillaries. Isolated capillaries were incubated for 30 min in medium containing 1 μM sulforhodamine 101 or 1 μM bodipy-ivermectin without (control) or with the indicated additions. Images were collected and analyzed as described under *Materials and Methods*. Data given as mean ± S.E. for 10 to 27 capillaries from one preparation. All additions significantly reduced luminal fluorescence ($P < .05$ for 0.01 μM ritonavir; $P < .01$ for all others).

Acknowledgments

We thank Destiny Sykes for excellent technical assistance.

References

Begley DJ, Lechardeur D, Chen ZD, Rollinson C, Bardoul M, Roux F, Scherman M and Abbott NJ (1996) Functional expression of P-glycoprotein in an immortalised cell line of rat brain endothelial cells, RBE4. *J Neurochem* **67:**988–995.

Drewe J, Gutmann H, Fricker G, Török M, Beglinger C and Huwyler J (2000) HIV protease inhibitor ritonavir: A more potent inhibitor of p-glycopotein than the cyclosporine analogue SDZ PSC-833. *Biochem Pharmacol*, in press.

Fricker G, Gutmann H, Droulle A, Drewe J and Miller DS (1999) Epithelial transport of anthelmintic ivermectin in a novel model of isolated proximal kidney tubules. *Pharm Res* **16:**1570–1575.

Glynn SL and Yazdanian M (1998) In vitro blood-brain barrier permeability of nevirapine compared to other HIV antiretroviral agents. *J Pharm Sci* **87:**306–310.

Golden PL and Pardridge WM (1999) P-glycoprotein on astrocyte foot processes of unfixed isolated human brain capillaries. *Brain Res* **819:**143–146.

Gutmann H, Fricker G, Drewe J, Toeroek M and Miller DS (1999a) Interactions of HIV protease inhibitors with ATP-dependent drug export proteins. *Mol Pharmacol* **56:**383–389.

Gutmann H, Fricker G, Torok M, Michael S, Beglinger S and Drewe J (1999b) Evidence for different ABC-transporters in Caco-2 cells modulating drug uptake. *Pharm Res* **16:**402–407.

Huai Yun H, Secrest DT, Mark KS, Carney D, Brandquist C, Elmquist WF and Miller DW (1998) Expression of multidrug resistance-associated protein (MRP) in brain microvessel endothelial cells. *Biochem Biophys Res Commun* **243:**816–820

Hegmann EJ, Bauer HC and Kerbel RS (1992) Expression and functional activity of P-glycoprotein in cultured cerebral capillary endothelial cells. *Cancer Res* **52:** 6969–6975.

Huwyler J, Drewe J, Klusemann C and Fricker G (1996) Evidence for P-glycoprotein-modulated penetration of morphine-6-glucuronide into brain capillary endothelium. *Br J Pharmacol* **118:**1879–1885.

Jette L, Tetu B and Beliveau R (1993) High levels of P-glycoprotein detected in isolated brain capillaries. *Biochim Biophys Acta* **1150:**147–154.

Kim RB, Fromm MF, Wandel C, Leake B, Wood AJ, Roden DM and Wilkinson GR (1998) The drug transporter P-glycoprotein limits oral absorption and brain entry of HIV1 protease inhibitors. *J Clin Invest* **101:**289–294.

Konig J, Nies AT, Cui Y, Leier I and Keppler D (1999) Conjugate export pumps of the multidrug resistance protein (MRP) family: Localization, substrate specificity and MRP2-mediated drug resistance. *Biochim Biophys Acta* **1461**:377–394.

Kusuhara H, Suzuki H, Naito M, Tsuruo T and Sugiyama Y (1998a) Characterization of efflux transport of organic anions in a mouse brain capillary endothelial cell line. *J Pharmacol Exp Ther* **285:**1260–1265.

Kusuhara H, Suzuki H and Sugiyama Y (1998b) The role of p-glycoprotein and canalicular multispecific organic anion transporter in the hepatobiliary excretion of drugs. *J Pharm Sci* **87:**1025–1040.

Mayer U, Wagenaar E, Dorobek B, Beijnen JH, Borst P and Schinkel AH (1997) Full blockade of intestinal P-glycoprotein and extensive inhibition of blood-brain barrier P-glycoprotein by oral treatment of mice with PSC833. *J Clin Invest* **100:** 2430–2436.

Masereeuw R, Russel FG and Miller DS (1996) Multiple pathways of organic anion secretion in renal proximal tubule revealed by confocal microscopy. *Am J Physiol* **271:**F1173–F1182.

Masereeuw R, Terlouw SA, van Aubel RAMH, Russel FGM and Miller DS (2000)

Endothelin B receptor-mediated regulation of ATP-driven drug secretion in renal proximal tubule. *Mol Pharmacol* 2000;57:59–67.
Miller DS (1995) Daunomycin secretion by killfish renal proximal tubules. *Am J Physiol* **269:**R370–R379.
Miller DS and Pritchard JB (1991) Indirect coupling of organic anion secretion to sodium in teleost (*Paralichthys lethostigma*) renal tubules. *Am J Physiol* **261:** R1470–R1477.
Pardridge WM (1998) Isolated brain capillaries: An in vitro model of blood-brain barrier research, in *Introduction to the Blood-Brain Barrier* (Pardridge WM ed) pp 49–61, Cambridge, Cambridge, UK.
Pardridge WM, Eisenberg J and Yamada T (1985) Rapid sequestration and degradation of somatostatin analogues by isolated brain microvessels. *J Neurochemistry* **44:**1178–1184.
Pardridge WM, Golden PL, Kang Y-S and Bickel U (1997) Brain microvascular and astrocyte localization of P-glycoprotein. *J Neurochem* **68:**1278–1285.
Regina A, Koman A, Piciotti M, El Hafney B, Center MS, Bergmann R, Courand P-O and Roux F (1998) Mrp1 multidrug resistance-associated protein and p-glycoprotein expression in rat brain microvessel endothelial cells. *J Neurochem* **71:**705–715.
Schaub TP, Kartenbeck J, Konig J, Vogel O, Witzgall R, Kriz W and Keppler D (1997) Expression of the conjugate export pump encoded by the mrp2 gene in the apical membrane of kidney proximal tubules. *J Am Soc Nephrol* **8:**1213–1221.
Schinkel AH, Smit JJ, Van Tellingen O, Beijnen JH, Wagenaar E, Van Deemter L, Mol CA, Van Der Valk MA, Robanus Maandag EC and Te Riele HP (1994) Disruption of the mouse mdr1a P-glycoprotein gene leads to a deficiency in the blood-brain barrier and to increased sensitivity to drugs. *Cell* **77:**491–502.
Schinkel AH, Wagenaar E, Mol CA and Van Deemter L (1996) P-glycoprotein in the blood-brain barrier of mice influences the brain penetration and pharmacological activity of many drugs. *J Clin Invest* **97:**2517–2524.
Schramm U, Fricker G, Wenger R and Miller DS (1995) P-glycoprotein-mediated secretion of a fluorescent cyclosporin analogue by teleost renal proximal tubules. *Am J Physiol* **268:**F46–F52.
Seetharaman S, Barrand MA, Maskell L and Scheper RJ (1998) Multidrug resistance-related transport proteins in isolated human brain microvessels and in cells cultured from these isolates. *J Neurochem* **70:**1151–1159.
Shirai A, Naito M, Tatasuta T, Dong J, Hanaoka K, Mikami K, Oh Hara T and Tsuruo T (1994) Transport of cyclosporin A across the brain capillary endothelial cell monolayer by P-glycoprotein. *Biochim Biophys Acta* **1222:**400–404.
Sullivan LP, Grantham JA, Rome L, Wallace D and Grantham JJ (1990) Fluorescein transport in isolated proximal tubules in vitro: Epifluorometric analysis. *Am J Physiol* **258:**F46–51.
Sussman I, Carson MP, McCall AL, Schultz V, Ruderman NB and Tornheim K (1988) Energy state of bovine cerebral microvessels: Comparison of isolation methods. *Microvasc Res* **35:**167–178.
Tatsuta T, Naito M, Oh Hara T, Sugawara I and Tsuruo T (1992) Functional involvement of P-glycoprotein in blood-brain barrier. *J Biol Chem* **267:**20383–20391.
Van Aubel RAMH, van Kuijck MA, Koenderink JB, Deen PMT, van Os CH and Russel FGM (1998) Adenosine triphosphate-dependent transport of anionic conjugates by the rabbit multidrug resistance-associated protein Mrp2 expressed in insect cells. *Mol Pharmacol* **53:**1062–1067.

Send reprint requests to: Dr. David S. Miller, LPC, NIH/NIEHS, P.O. Box 12233, Research Triangle Park, NC 27709. E-mail: miller@niehs.nih.gov